



**HAL**  
open science

## CO<sub>2</sub> Solubility Modelling in Non-Precipitating Aqueous Solutions of Potassium Lysinate

Antonio Conversano, Serena Delgado, Christophe Coquelet, Stefano Consonni,  
Manuele Gatti

► **To cite this version:**

Antonio Conversano, Serena Delgado, Christophe Coquelet, Stefano Consonni, Manuele Gatti. CO<sub>2</sub> Solubility Modelling in Non-Precipitating Aqueous Solutions of Potassium Lysinate. *Separation and Purification Technology*, 2022, 300, pp.121855. 10.1016/j.seppur.2022.121855 . hal-03751942

**HAL Id: hal-03751942**

**<https://hal.science/hal-03751942>**

Submitted on 16 Aug 2022

**HAL** is a multi-disciplinary open access archive for the deposit and dissemination of scientific research documents, whether they are published or not. The documents may come from teaching and research institutions in France or abroad, or from public or private research centers.

L'archive ouverte pluridisciplinaire **HAL**, est destinée au dépôt et à la diffusion de documents scientifiques de niveau recherche, publiés ou non, émanant des établissements d'enseignement et de recherche français ou étrangers, des laboratoires publics ou privés.

# CO<sub>2</sub> Solubility Modelling in Non-Precipitating Aqueous Solutions of Potassium Lysinate

Antonio Conversano<sup>a,b</sup>, Serena Delgado<sup>c,d</sup>, Christophe Coquelet<sup>c,e\*</sup>, Stefano Consonni<sup>a,b</sup>, Manuele Gatti<sup>a</sup>

<sup>a</sup> Dipartimento di Energia, Politecnico di Milano, via Lambruschini 4, 20156 Milano, Italia

<sup>b</sup> LEAP-Laboratorio Energia ed Ambiente Piacenza, via Nino Bixio 27/C, 29121 Piacenza, Italia

<sup>c</sup> Mines ParisTech, PSL University, Centre of Thermodynamics of Processes (CTP), 35, rue Saint Honoré, 77305 Fontainebleau cedex, France

<sup>d</sup> TotalEnergies Tour Coupole, La Défense, 2 Pl. de la Coupole-Jean Millier, 92400

<sup>e</sup> Université de Toulouse, Mines Albi, Centre RAPSODEE UMR CNRS 5302, Campus Jarlard, Albi, France

\*corresponding author: christophe.coquelet@mines-paristech.fr

---

## ABSTRACT

Modelling of CO<sub>2</sub> solubility in aqueous solutions of potassium lysinate (LysK) is mainly hindered by scarcity of experimental vapor-liquid equilibrium data and lack of chemical equilibrium constants associated to the reaction mechanism for the CO<sub>2</sub>/LysK/H<sub>2</sub>O system. Therefore, Kent-Eisenberg (KE) correlation stands out from the literature, being among the most used approaches for the description of the equilibrium CO<sub>2</sub> partial pressure at different loadings. In this work, a Kent-Eisenberg-like approach has been developed, enhancing the empirical Kent-Eisenberg with Debye-Hückel activity coefficients in order to guide model calibration with reference to selected experimental data for CO<sub>2</sub> solubility in 33.1 and 33.5%<sub>w/w</sub> aqueous LysK solution; moreover, the KE edition provides an estimation of the missing equilibrium constants. This information has been embedded in a first thermodynamically sound and predictive Deshmukh-Mather (DM) model (average absolute deviation equal to 7%) validated against additional experimental data in a wide temperature and concentration range.

---

## 1. Introduction

Global economy expansion in 2018 has been associated with a contextual increase in energy demand, recording 2.3% incremental consumption with respect to 2017. As a result, energy-related CO<sub>2</sub> emissions reached a historic high of 33.1 GtCO<sub>2</sub> in the same reference year, with 30% of emissions due to coal fire power generation being the single largest emitter<sup>1</sup>. Overall, the power sector accounted for nearly two-thirds of emissions growth. With reference to 2017, 2018 has seen an estimated 4.6% natural gas consumption increase because of the rise in energy requirement and as a consequence of the progressive coal-to-gas switch, which has contributed for almost 60 Mt of avoided coal and consequent saving of 95 MtCO<sub>2</sub>/y<sub>2018</sub>.

To meet the goals of the Paris agreement aiming at an increase in global average temperature “well below” 2°C above pre-industrial levels, the clean energy transition will need to bring about a rapid reduction of greenhouse gases down to net zero CO<sub>2</sub> emissions by the second half of the century. To this end, no single path can be identified. However, the strategic portfolio recommended by researchers and intergovernmental organizations quantifies the role of Carbon Capture, Utilization and Storage (CCUS) technologies to 15% CO<sub>2</sub> of emission savings in 2070<sup>2</sup>.

Among the capture technologies, Post Combustion Capture (PCC) is a mature and retrofittable option for CO<sub>2</sub> capture from flue gas for power industry decarbonization. In case of low CO<sub>2</sub> partial pressure in the treated gas stream, PCC-scrubbing with solvents involves CO<sub>2</sub>-sorbent chemical reaction, which forms weakly bonded intermediate compounds to be regenerated. This step restores the solvent and releases an isolated CO<sub>2</sub>-rich stream ready for dehydration, compression, and storage. PCC-chemical scrubbing has high removal rate and selectivity<sup>3</sup>. Specifically, aqueous monoethanolamine (MEA) at 30%<sub>w/w</sub> has been taken as a benchmark in several European initiatives focusing on Natural Gas Combined Cycle (NGCC)-flue gas decarbonisation (e.g. projects<sup>4,5</sup>). However, MEA scrubbing shows many drawbacks; among these, high-energy consumption for regeneration, limited CO<sub>2</sub> loading capacity, equipment corrosion and elevated packed volumes of the absorption unit, generation of toxic compounds and amine volatility constitute areas of improvement.

46 Therefore, new studies on alternative solvents focus on identifying more effective, energy saving and greener  
47 solvents for a low-carbon energy production industry. With these regards, amino acid salts (AAS) solutions  
48 are attracting the attention of the scientific community working on CO<sub>2</sub> capture<sup>6</sup>: they present the same  
49 functional amino group as alkanolamines, they can reach high CO<sub>2</sub> loading capacity and fast reaction rates;  
50 moreover, they are considered environmentally friendly, showing low volatility and ecotoxicity, stability  
51 against oxidation, together with negligible corrosion effects<sup>7,8</sup>.

52 Research activities on amino acid salts solutions for CO<sub>2</sub> absorption are already ongoing. An important work  
53 has been carried out by Siemens Company, which has proposed a carbon capture process known as  
54 “POSTCAP”, tested at pilot scale<sup>9</sup> and modelled to predict the specific thermal energy demand for solvent  
55 regeneration in case of a full-scale capture unit. The POSTCAP technology applied to a coal-fired reference  
56 power plant is estimated to require 2.7 MJ/kgCO<sub>2</sub> captured<sup>9</sup> versus a reference value of 3.7 MJ/kgCO<sub>2</sub> for the  
57 benchmark solvent (30%<sub>w/w</sub> MEA solutions).

58 Literature review, experimental campaigns and data analysis to quantify the absorption potential of selected  
59 amino acid salts solutions in NGCC-CO<sub>2</sub> capture applications have been carried out by the authors<sup>10,11</sup>. From  
60 this screening, potassium lysinate (LysK) has been identified as a relevant compound due to its high capacity  
61 and loading, fast kinetics and significant CO<sub>2</sub> absorption flux. Therefore, further investigation on its potential  
62 as a greener option in PCC-scrubbing applications is necessary, requiring vapour-liquid equilibria (VLE)  
63 measurements and thermodynamic modelling, CO<sub>2</sub> capture unit design and techno-economic assessment (to  
64 quantify e.g., specific reboiler thermal duty required for regeneration, SPECCA index, cost of electricity,  
65 cost of CO<sub>2</sub> avoided).

66 The availability of reliable and accurate information on carbon dioxide equilibrium solubility in aqueous  
67 solutions of AAS is of paramount importance to proper design gas treating units. In this area, the literature  
68 offers a variety of works mainly based on Kent-Eisenberg (KE) correlation<sup>12-18</sup>, with ideal mixture  
69 assumption. This framework makes Kent-Eisenberg regressions unfit for extrapolation. Hence, researchers  
70 working on CO<sub>2</sub> solubility in aqueous amines have moved towards the application of activity coefficient  
71 models such as the electrolyte-NRTL (e-NRTL) model from Chen and Evans<sup>19</sup>, and the Deshmukh-Mather  
72 model<sup>20</sup>, which provide greater rigor and a more thermodynamically-sound methodology.

73 Although both solutions account for long- and short-range particle interactions, Deshmukh-Mather has  
74 demonstrated accuracy and reliability with a computationally affordable price and a simple activity  
75 coefficient expression. Kent-Eisenberg is state-of-the-art for the description of the AAS/CO<sub>2</sub>/H<sub>2</sub>O systems,  
76 and is extensively adopted, although very recent publications for different amino acid salts-based systems  
77 (e.g., potassium taurate) have applied the e-NRTL model<sup>21</sup> in Aspen<sup>®</sup> simulator. In the specific case of CO<sub>2</sub>  
78 solubility in aqueous potassium lysinate solutions, VLE description still relies on empirical correlations  
79 (KE), hence constituting a relevant case-study for more rigorous thermodynamic modelling. Nevertheless,  
80 unavailable chemical equilibrium constant parameters are still estimated with KE.

81 This work is meant to fill the gap, proposing a first semi-empirical thermodynamic model for CO<sub>2</sub> solubility  
82 in the non-precipitating LysK/CO<sub>2</sub>/H<sub>2</sub>O system. The model has been coded in Matlab<sup>®</sup> using Deshmukh-  
83 Mather formulation, while starting from a modified edition of the Kent-Eisenberg correlation (i.e., Kent-  
84 Eisenberg endowed with Debye-Hückel activity coefficient expression) used to identify missing carbamate  
85 hydrolysis equilibrium constants. The Deshmukh-Mather approach has been selected because of its compact  
86 activity coefficient model expression. A comparison against other models with more sophisticated activity  
87 coefficient formulations (e.g., e-NRTL) would be beneficial and will be carried out in future works.  
88 Moreover, further experimental investigation of vapour-liquid equilibrium of CO<sub>2</sub> in aqueous LysK solution  
89 need to be performed to validate the model over a wider loading range compared to the one characterizing  
90 the here-identified literature data. Finally, experiments are required for a complete identification of the set of  
91 equilibrium constants.

92 The manuscript is organized as follows: Section 2 defines the thermodynamic problem. It is followed by a  
93 description of the used methodology (Section 3) which has allowed the transition from the empirical Kent-

94 Eisenberg correlation to its formulation which includes activity coefficients; this sets the ground for the  
95 Deshmukh-Mather model definition. Results and discussion are reported in Section 4 while conclusion and  
96 perspectives for further the investigation<sup>22</sup> are mentioned in Section 5.

97

## 98 **2. Thermodynamic Framework**

### 99 **2.1. Rationale**

100 An appropriate thermodynamic model needs to give an extensive description of CO<sub>2</sub> solubility partial  
101 pressure as a function of loading, temperature, and concentration. It should also accurately predict other  
102 thermodynamic properties required in energy balance calculations, such as solvent enthalpies, entropies, etc.  
103 Models are not completely predictive in nature, and they usually rely on experimental data to provide good  
104 correlations. In the literature, it is common to distinguish empirical and semi-empirical (or rigorous) models.  
105 The first category includes models consisting in mathematical correlations; they may assume liquid and  
106 vapour phase ideal behaviour (which is a strong assumption) with weak or no theoretical background.  
107 Common empirical models sometimes lump system non ideality within correction factors or model  
108 parameters regressed against experimental data, providing quite reliable yet simple correlations valid within  
109 the regression interval of temperature and composition, with consequent accuracy reduction outside of this  
110 range. Although modifications could provide accuracy improvements, the intrinsic limitation given by the  
111 phase ideality assumption can be detrimental to the validity of this empirical approach, paving the way for  
112 rigorous models such as excess Gibbs energy ( $G^E$ ), equation of state (EoS) and their combination (EoS/ $G^E$ ).  
113 Semi-empirical models are based on the equivalence of single component fugacity in vapour and liquid  
114 phase. Sophisticated formulations require the use of equation of state for the gas phase, and an activity  
115 coefficient model for the liquid phase, leading to an effective representation of CO<sub>2</sub> solubility in liquid  
116 solution for a wide range of operating process parameters because of an increase in model complexity.  
117 Nevertheless, rigorous models remain semi-empirical as they adopt calibrated parameters that are tuned  
118 against experimental data to guarantee both accuracy in the calibration range and effective prediction outside  
119 of it<sup>23</sup>.

120 As previously mentioned, a very common empirical correlation used in the industry to describe CO<sub>2</sub>  
121 solubility in amine solutions is the Kent-Eisenberg correlation (discussed in Paragraph 2.3). Kent-Eisenberg  
122 approach assumes ideal liquid and gas phases. In previous literature work, the non-ideal behaviour of the  
123 system is lumped within the calibrated protonation and carbamate hydrolysis reaction parameters. Therefore,  
124 KE assumes that the equilibrium constants are functions of concentration and temperature only, with unitary  
125 activity coefficients. The model provides a fair fitting within the calibration interval, but it does not involve  
126 any theoretical formulation that justifies extrapolation.

127 Semi-empirical models rigorously calculate system non-ideality by including activity coefficients within the  
128 equilibrium constants. Among the most relevant formulations, Deshmukh and Mather have proposed a model  
129 based on the Guggenheim activity coefficient equation, which is a combination of a first term accounting for  
130 long-range interactions (electrostatic forces as described by Debye-Hückel) and a second term expressing  
131 short range interactions (for more details, Paragraph 2.4).

132 e-NRTL is an extension of the NRTL model<sup>24</sup> that calculates liquid activity coefficients. This model has  
133 been initially proposed for aqueous electrolyte systems<sup>19</sup> but it has been extended for mixed-solvent  
134 electrolyte systems. The activity coefficients obtained from this thermodynamic formulation stem from three  
135 contributions, namely a Pitzer-Debye-Hückel (PDH) term, a Born term and a NRTL term. PDH is an  
136 unsymmetrical normalised contribution proposed by Pitzer<sup>25</sup> for long-range ion-ion interactions existing  
137 beyond the immediate neighbourhood of a central ionic species. The Born term is the unsymmetrical  
138 normalised contribution<sup>26</sup> accounting for the effect of mixed solvent. It expresses the difference in Gibbs free  
139 energy between ionic species in a mixed solvent and in water. The last contribution is the unsymmetrical  
140 NRTL normalised contribution related to local interaction in the immediate neighbourhood of any central  
141 species. Several examples of e-NRTL model application can be found in the literature: Austgen has  
142 represented the vapour-liquid equilibria of acid gas in diethanolamine (DEA) and MEA solutions<sup>27</sup>, Borhani

143 has adopted the model to compare equilibrium and non-equilibrium process models for tray column, also  
144 comparing the effect of different amines as promoters on potassium carbonate process<sup>28</sup>, Hilliard has  
145 completed several thermodynamic models representing CO<sub>2</sub> solubility with amine solvent, dedicating special  
146 efforts to aqueous MEA<sup>29</sup>.

147 The extended universal quasi-chemical functional group activity coefficient electrolyte model<sup>30</sup> (e-  
148 UNIQUAC) is an additional semi-empirical model that is built upon the UNIQUAC formulation. The e-  
149 UNIQUAC excess Gibbs energy expression contains a combinatorial or entropic term accounting for short-  
150 range ion-ion interactions. This term only depends on the size of the species, regardless of system  
151 temperature. The second residual or enthalpic term for short-range ion-ion interactions is temperature-  
152 dependent. Moreover, the additional contribution of the e-UNIQUAC formulation with respect to the  
153 UNIQUAC expression is given by a third Debye-Hückel term which accounts for long-range electrostatic  
154 interactions. Significant literature adopting e-UNIQUAC model refers to CO<sub>2</sub> solubility description for  
155 aqueous MEA solutions carried out by Aronu et al.<sup>31</sup> Other examples include its application for the  
156 thermodynamic representation of carbon dioxide absorption in aqueous MEA and methyldiethanolamine  
157 (MDEA) solutions by Faramarzi et al.<sup>32</sup>.

158 In case sufficient data are not available, a possible solution for solubility description is the UNIFAC model,  
159 which is a group contribution method presented by Fredenslund et al.<sup>33</sup> The model has been used by Ye et al.  
160 to predict vapour liquid equilibria and vapour liquid-liquid equilibria for systems constituted by methanol  
161 (MeOH), dimethyl ether (DME), CO<sub>2</sub> and H<sub>2</sub>O<sup>34</sup>. It predicts the activity coefficients by adding a  
162 combinatorial and residual term, averaging group-group interactions of the selected molecules.

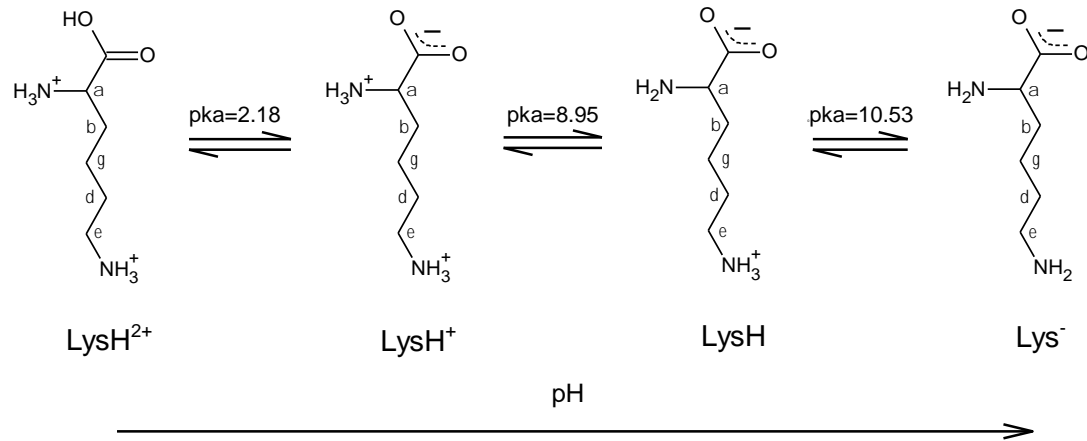
163 In the present application, the rigorous Deshmukh-Mather model has been selected and fully implemented in  
164 Matlab<sup>®</sup> as it provides higher accuracy in terms of solubility description with respect to the empirical Kent-  
165 Eisenberg approach and reduced computational effort compared to e.g., e-NRTL<sup>35</sup>.

166

## 167 **2.2. The thermodynamic problem of the CO<sub>2</sub>/LysK/H<sub>2</sub>O system**

168 The amino acid salt considered in this work is potassium lysinate (LysK), which has been assessed in the  
169 perspective of CO<sub>2</sub> post combustion capture applications via non-precipitating chemical absorption. This  
170 choice stems from preliminary results of previous experimental activities at laboratory<sup>36-38</sup> and bench-scale<sup>39</sup>.  
171 Solvent selection relies on mass transfer and energy performance indicators. A solvent selection screening  
172 methodology has been investigated in previous work<sup>11,39</sup>.

173 From a chemical standpoint, lysine is an organic molecule with one carboxyl group in  $\alpha$  position (pKa=2.18  
174 at 25°C), and two amino groups respectively in  $\alpha$  (pKa=8.95 at 25°C) and in  $\epsilon$  (pKa=10.53 at 25°C)  
175 positions<sup>40</sup>. In aqueous solution, Lysine dissociates differently depending on the pH: as represented in Figure  
176 1, the anionic form Lys<sup>-</sup> is prevalent at high pH, shifting towards LysH (zwitterionic form) which reaches its  
177 highest concentration at the isoelectric point (pI). In acidic solution, LysH<sup>+</sup> (cationic form) and LysH<sup>2+</sup> (di-  
178 cationic form) are the prevalent species<sup>41-43</sup>.



179

180

Figure 1: Ionization equilibria of lysine in water-based solutions at 25°C.

181 Given the presence of amino functional groups, CO<sub>2</sub> is expected to react directly or through an acid-base  
 182 buffer mechanism with AAS, forming non-volatile ionic species, as with alkanolamines<sup>27,44</sup>

183 *Carbamate hydrolysis reactions:*



184 *Dissociation of protonated amino acid:*



185 *Hydrolysis of carbon dioxide:*



186 *Dissociation of bicarbonate:*



187 *Dissociation of water:*



188 Where  $\text{CARB1} = \text{NH}_3^+ - \text{R}_2\text{R}_1\text{CH} - \text{NHCOO}^-$ ,  $\text{CARB2} = ^-\text{OOC}^-\text{HN} - \text{R}_2\text{R}_1\text{CH} - \text{NH}_2$ ,  $\text{R}_1 = -\text{COO}^-$  and  
 189  $\text{R}_2 = -(\text{CH}_2)_4 -$ ,  $\text{LysH} = \text{NH}_3^+ - \text{R}_2\text{R}_1\text{CH} - \text{NH}_2$  and  $\text{Lys}^- = \text{NH}_2 - \text{R}_2\text{R}_1\text{CH} - \text{NH}_2$ .

190 Chemical equilibrium is then represented by equilibrium equations (Eq. 8-Eq. 14) considered relevant for the  
 191 description of CO<sub>2</sub> solubility in aqueous non-precipitating LysK solutions<sup>44</sup>:

$$K_{R1} = \frac{\ddot{a}_{\text{LysH}} \ddot{a}_{\text{HCO}_3^-}}{\ddot{a}_{\text{CARB1}} \ddot{a}_{\text{H}_2\text{O}}} \quad \text{Eq. 8}$$

$$K_{R2} = \frac{\ddot{a}_{\text{Lys}^-} \ddot{a}_{\text{HCO}_3^-}}{\ddot{a}_{\text{CARB2}} \ddot{a}_{\text{H}_2\text{O}}} \quad \text{Eq. 9}$$

$$K_{\text{LysH}^+} = \frac{\ddot{a}_{\text{H}^+} \ddot{a}_{\text{LysH}}}{\ddot{a}_{\text{LysH}^+}} \quad \text{Eq. 10}$$

$$K_{\text{LysH}} = \frac{\ddot{a}_{\text{H}^+} \ddot{a}_{\text{Lys}^-}}{\ddot{a}_{\text{LysH}}} \quad \text{Eq. 11}$$

$$K_{\text{CO}_2} = \frac{\bar{a}_{\text{H}^+} \bar{a}_{\text{HCO}_3^-}}{\bar{a}_{\text{CO}_2} a_{\text{H}_2\text{O}}} \quad \text{Eq. 12}$$

$$K_{\text{HCO}_3^-} = \frac{\bar{a}_{\text{H}^+} \bar{a}_{\text{CO}_3^{2-}}}{\bar{a}_{\text{HCO}_3^-}} \quad \text{Eq. 13}$$

$$K_{\text{H}_2\text{O}} = \frac{\bar{a}_{\text{H}^+} \bar{a}_{\text{OH}^-}}{a_{\text{H}_2\text{O}}} \quad \text{Eq. 14}$$

192 Speciation constraints are added to the chemical equilibria equations: amino acid balance, CO<sub>2</sub> balance, total  
 193 balance and charge balance (Eq. 15-Eq. 18). The system of equations to solve for the liquid-phase speciation  
 194 consists in Eq. 8-Eq. 18.

$$n_{\text{LysH}|_0} = n_{\text{LysH}} + n_{\text{LysH}^+} + n_{\text{Lys}^-} + n_{\text{CARB1}} + n_{\text{CARB2}} \quad \text{Eq. 15}$$

$$\alpha n_{\text{LysH}|_0} = n_{\text{CO}_2} + n_{\text{CARB1}} + n_{\text{CARB2}} + n_{\text{CO}_3^{2-}} + n_{\text{HCO}_3^-} \quad \text{Eq. 16}$$

$$\sum_{i=1}^c x_i = 1 \quad \text{Eq. 17}$$

$$n_{\text{K}^+} + n_{\text{H}^+} + n_{\text{LysH}^+} = n_{\text{Lys}^-} + 2n_{\text{CARB2}} + n_{\text{CARB1}} + 2n_{\text{CO}_3^{2-}} + n_{\text{HCO}_3^-} + n_{\text{OH}^-} \quad \text{Eq. 18}$$

195 Where  $n_{\text{LysH}|_0} = n_{\text{LysK}|_0}$  is the lysinate apparent mole number in liquid phase and  $\alpha$  is the CO<sub>2</sub> loading  
 196 (molCO<sub>2</sub>/mol LysK) and  $n_i$  is the mole number of component  $i$ . Using a stoichiometric approach, this system  
 197 of equations has been solved with successive substitutions based on the Newton-Raphson method.

198

### 199 2.3. Kent-Eisenberg Correlation

200 Kent-Eisenberg model is a widely-used empirical thermodynamic model in the field of acid gas absorption<sup>45</sup>  
 201 to describe CO<sub>2</sub> vapour-liquid equilibria in aqueous alkanolamine solutions. The chemical reactions  
 202 equilibrium constants are usually available from the literature, except for carbamation and protonation  
 203 reactions of amines expressed as a temperature-dependent functional form and coefficients used as tuning  
 204 parameters for data fitting. Consequently, apparent equilibrium constants embed system non ideality and  
 205 activity coefficients are set to unity due to the ideal solution assumption<sup>13</sup>.

206 Several applications and modifications of the Kent-Eisenberg model are recorded in the literature. Among  
 207 these, Jou et al.<sup>46</sup> limit the tuning parameters of the equilibrium constants to the protonation equations only,  
 208 varying their functional equation with a dependence on temperature, alkanolamine concentration and  
 209 pressure. Hu and Chakma<sup>47,48</sup> assume apparent equilibrium constant for AMP and DGA protonation to  
 210 depend on liquid-phase gas concentration and alkanolamine concentration. Li and Shen<sup>49</sup> introduce a  
 211 correction of the chemical equilibrium constants composed of a temperature-dependent factor multiplied by  
 212 an activity-dependent-based constant, which is a function of loading, amine concentration and includes  
 213 tuneable parameters. This last contribution has been debated in the literature<sup>13</sup> as the use of loading in  
 214 activity coefficient-based equilibrium contribution affects the model's predictive capabilities.

215 To further simplify the iterative approach initially proposed by Kent and Eisenberg, a mathematical  
 216 algorithm has been introduced by Haji-Sulaiman et al. in 1998<sup>50</sup> to solve the thermodynamic problem with a  
 217 single polynomial equation as a function of hydrogen ion concentration. The selected root belongs to a pH  
 218 interval of 7-11 and it can be used to determine speciation.

219 Successive KE modifications in the literature propose different apparent equilibrium constant expressions,  
 220 which attempt to reproduce the composition dependency properly belonging to the activity coefficients  
 221 formulation that is neglected by assumption<sup>51</sup>. This simple approach has been widely spread and adopted by  
 222 the industry, however modelling results highlight that KE provides satisfactory performance for medium  
 223 loadings only, presenting higher deviations in the low and high loading range. In addition to this, KE is not  
 224 thermodynamically-sound, and it is intrinsically not predictive due to the lack of activity coefficients.

225 In the present investigation, a revised KE model is proposed and calibrated against a dataset constituted by  
 226 VLE data at 33.1 %<sub>w/w</sub> LysK concentration at absorber conditions<sup>44</sup> and VLE data at 33.5 %<sub>w/w</sub> LysK  
 227 concentration at stripper conditions<sup>52</sup>. This dataset has been selected as it covers a fair loading range (0.5 –  
 228 1.5 molCO<sub>2</sub>/molLysK) compared to other experimental literature data, and a broad temperature window (298  
 229 K – 393 K). Moreover, the selected dataset shows reduced data dispersion (see supplementary material for  
 230 further details on identified datasets).

231 KE adoption has been necessary to compensate missing equilibrium constants, i.e. carbamate hydrolysis and  
 232 amino acid protonation from the set of equations Eq. 8 – Eq. 14. With respect to equilibrium constants  
 233 referred to protonated AAS dissociation, experimental data from Nagai et al.<sup>53</sup> have been interpolated in a  
 234 temperature range spanning from 283.1 K to 333.1 K. Consequently, coefficients for temperature-dependent  
 235 equilibrium constant of carbamate hydrolysis reactions have been estimated by VLE data regression.  
 236 Moreover, the edition of the KE correlation proposed for this study is endowed with an activity coefficient  
 237 model based on Debye–Hückel formulation (Paragraph 2.4). Debye–Hückel limiting law describes non-ideal  
 238 behaviour due to electrostatic forces in extremely dilute electrolyte solutions<sup>54</sup>. Therefore, while regressing  
 239 the missing equilibrium constants, this revised KE version is expected to provide reasonable extrapolation of  
 240 the vapour-liquid equilibria in a lower loading range, steering KE outside its calibration range.

241 In line with the recent literature on the topic, ideal gas phase has been assumed and CO<sub>2</sub> phase equilibrium  
 242 has been described using Henry’s law ( $\hat{\phi}_{CO_2}^V$  and Poynting factor further discussed in the supplementary  
 243 material are set to 1).

244 Within this framework, the revised KE is propaedeutic to the definition of a related Deshmukh-Mather  
 245 model as (i) it requires the selection of a robust dataset for model calibration and (ii) the equilibrium  
 246 constants (related to the two carbamate hydrolysis reactions) estimated within the KE framework can be  
 247 embedded in the Deshmukh-Mather model.

248 Figure 2 reports a scheme of the adopted revised Kent-Eisenberg approach. The model has been  
 249 implemented in Matlab<sup>®</sup> and the temperature-dependent coefficients of the apparent equilibrium constants  
 250 minimise the selected objective function with Matlab<sup>®</sup> fminsearch function. The objective function  $F_{obj}$   
 251 minimised during the parameter regression is reported in Eq.19 and it accounts for the deviation between  
 252 experimental and modelled CO<sub>2</sub> partial pressure. Results of the regression against experimental data are  
 253 reported in Table 1, meanwhile identified equilibrium constants used to solve the thermodynamic problem  
 254 are reported in Section 4.

$$F_{obj} = \sum_{i=1}^n \left( \frac{p_{CO_2,i}^{Exp} - p_{CO_2,i}^{Model}}{p_{CO_2,i}^{Exp}} \right)^2 \quad Eq. 19$$

Table 1: Kent-Eisenberg correlation regression against Shen’s VLE data set.

Equilibrium constants	Cf. Section 4		
Experimental dataset (Shen et al. <sup>44</sup> and Li et al. <sup>52</sup> )	<b>N. experimental data</b>	97	[-]
	<b>Temperature range</b>	298-393	K
	<b>Loading range</b>	0.5 – 1.5	molCO <sub>2</sub> / molLysK
<b>Tolerance</b>	1.00E-04		[-]
<b>Average absolute deviation – AAD%<sup>†</sup></b>	9		%

$$^{\dagger}AAD = 100 \frac{\sum_{i=1}^n \left| \frac{p_{CO_2,i}^{Exp} - p_{CO_2,i}^{Model}}{p_{CO_2,i}^{Exp}} \right|}{n} [\%]$$



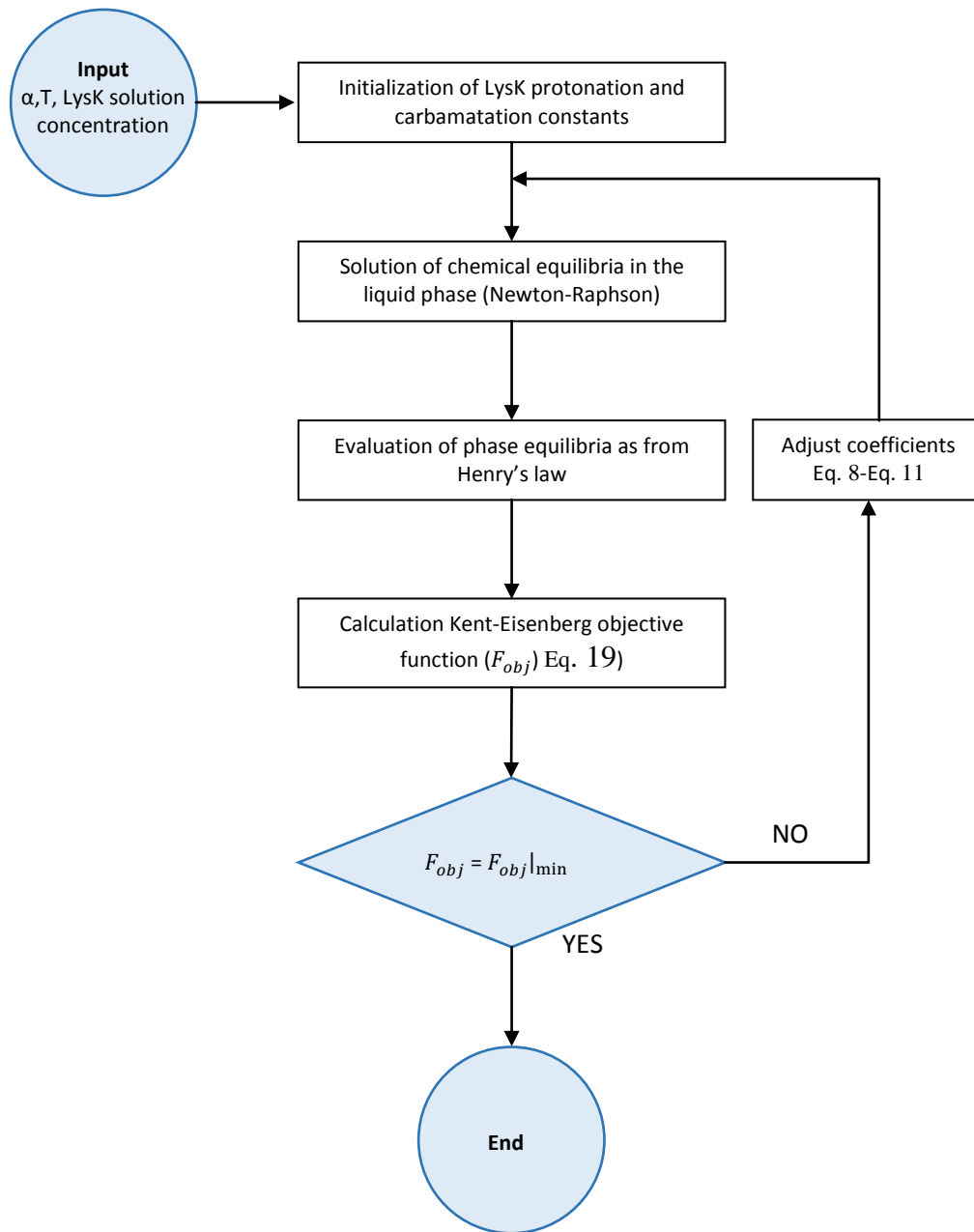


Figure 2: Revised Kent-Eisenberg algorithm.

258

259

260

261

#### 2.4. Deshmukh-Mather Model

262 The Deshmukh-Mather model calculates the excess Gibbs free energy using the activity coefficient equation  
 263 proposed by Guggenheim and Stokes<sup>55</sup>, which is essentially an extension of the Debye-Hückel model. The  
 264 corresponding activity coefficient equation (Eq. 20) consists in a first term expressing the Debye-Hückel law  
 265 accounting for the electrostatic forces, and a second and correlative term which is added to consider short-  
 266 range van der Waals interactions. The adjusted parameters in this model are the  $r_i$  length in the Debye-  
 267 Hückel term (in Å; comparable to an ion radius), and the  $\beta_{ij}$  binary interaction coefficients (in kg H<sub>2</sub>O/mol).

$$\ln \tilde{\gamma}_i = -\frac{Az_i^2 I^{1/2}}{1 + Br_i I^{1/2}} + 2 \sum_j \beta_{ij} m_j \quad \text{Eq. 20}$$

268 Where  $z_i$  is the component charge number,  $m_i$  its molality (mol/kg H<sub>2</sub>O), and  $I = \frac{1}{2} \sum_j z_j^2 m_j$  is the molality-  
269 scale ionic force (mol/kg H<sub>2</sub>O).

270 Parameters used in the Deshmukh-Mather model can be found in the Supplementary Materials. A  
271 conventional formulation of the  $\beta_{ij}$  term from the Guggenheim equation is showed in Eq. 21.

$$\beta_{ij} = a_{ij} + b_{ij}T \quad \text{Eq. 21}$$

272 The DM model developed to describe CO<sub>2</sub> solubility in LysK aqueous solutions is based on the following  
273 assumptions: **(i)** the model inherits the equilibrium constants coefficients provided by VLE data regression  
274 from KE; **(ii)** DM calibration has been carried out by tuning parameters  $a_{ij}$  and  $b_{ij}$  against the same VLE  
275 dataset used for KE.

276 The DM regression algorithm and objective functions are consistent with the ones reported in Figure 2 for  
277 KE. Results of the regression to identify binary interaction parameters  $\beta_{ij}$  are reported in Section 4. The  
278 solution scheme of the liquid-phase chemical reaction system and of the vapour-liquid equilibria is reported  
279 in Figure 3.

280  
281  
282  
283  
284  
285  
286  
287  
288  
289  
290  
291  
292  
293  
294  
295  
296  
297  
298  
299  
300  
301

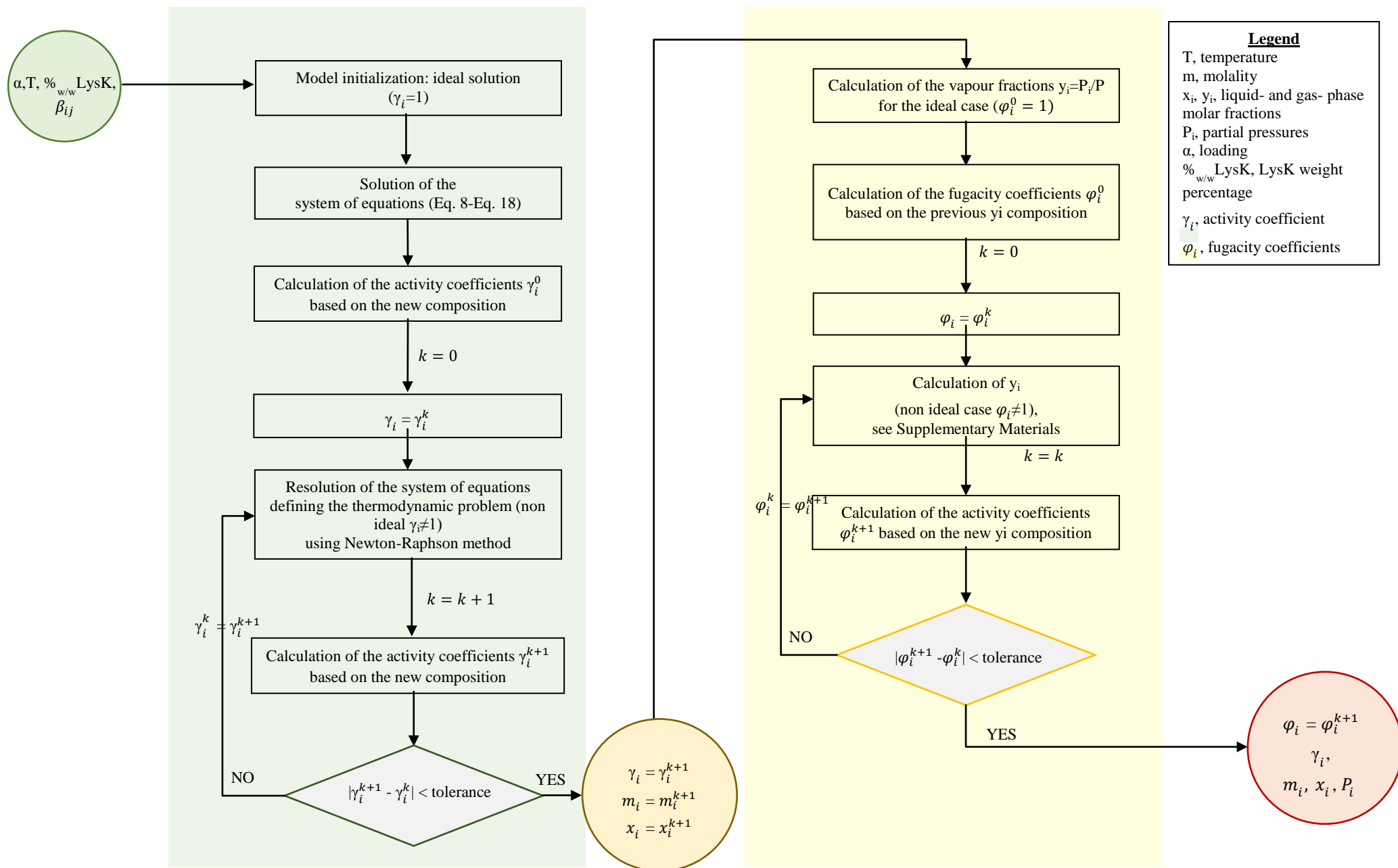


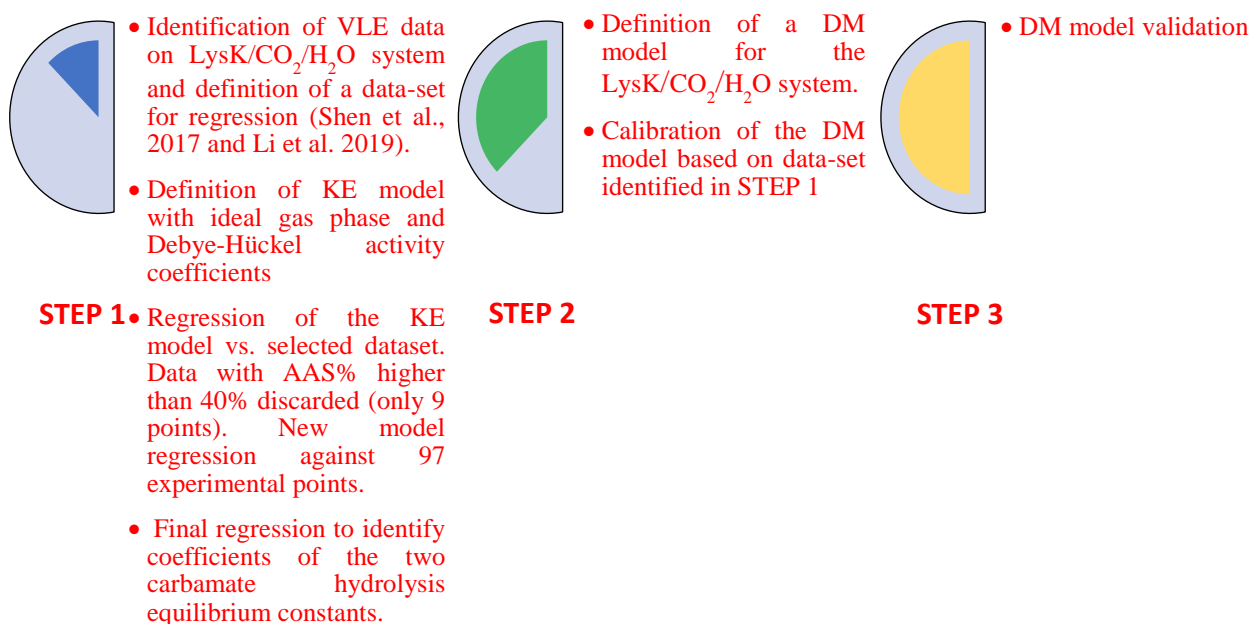
Figure 3: Main algorithm describing DM model.

### 302 3. Approach and Methodology

303 Within the present work, a thermodynamic model of CO<sub>2</sub> solubility in the alternative aqueous LysK solvent  
304 has been developed starting from an enhanced Kent-Eisenberg correlation calibrated for 33.1 and 33.5%<sub>w/w</sub>  
305 aqueous LysK VLE data from Shen et al.<sup>44</sup> and Li et al.<sup>52</sup>. Model calibration has been carried out selecting  
306 data among the highest available concentrations from the literature<sup>44,52,56</sup>, as recommended in previous work  
307 assessing solvent capacity against a reference commercial solvent (i.e., 30%<sub>w/w</sub> MEA aqueous solution) at  
308 bench-scale<sup>6,39</sup> for NGCC-flue gas decarbonisation (i.e., ~4% CO<sub>2</sub> molar fraction in the flue gas). Moreover,  
309 the selected data set is characterized by consistent data in a wide loading and temperature range and it has  
310 been identified among a number of different literature sources<sup>37,44,52,57-61</sup>.

311 KE modelling results are twofold: a complete set of constants representative of the investigated system is  
312 identified after regression against VLE data for LysK solutions at 33.1%<sub>w/w</sub> and 33.5%<sub>w/w</sub>, loading between  
313 0.5 - 1.5 molCO<sub>2</sub>/molLysK and a temperature range of 298.1 – 393.1 K, representative of absorption and  
314 stripping conditions. Moreover, a novel KE formulation endowed with Debye-Hückel activity coefficients  
315 has been developed. Although based on regression, the set of equilibrium constants defined from KE-model  
316 can be embedded in a thermodynamically sound Deshmukh-Mather model describing CO<sub>2</sub> solubility in  
317 aqueous LysK solutions. Deshmukh-Mather parameter regression over the selected dataset has been carried  
318 out over the same data set used for KE regression, tuning  $\beta_{ij}$  terms. Species pairs to investigate have been  
319 selected as from Weiland et al.<sup>62</sup>: interactions between like-charged ions are discarded, as well as molecule  
320 self-interactions (excluding MEA) and interactions between water and its ionization products. Further,  
321 interactions between the acid gas and other components have been disregarded. Results of KE correlation,  
322 equilibrium constant parameters, Deshmukh-Mather model, and adjusted binary interaction parameters are  
323 described in Section 4. A visual summary of the methodology is shown in Figure 4.

324



325

326 *Figure 4: Main steps leading to the definition of a Deshmukh-Mather model for the LysK/CO<sub>2</sub>/H<sub>2</sub>O system.*

### 327 4. Results and Discussion

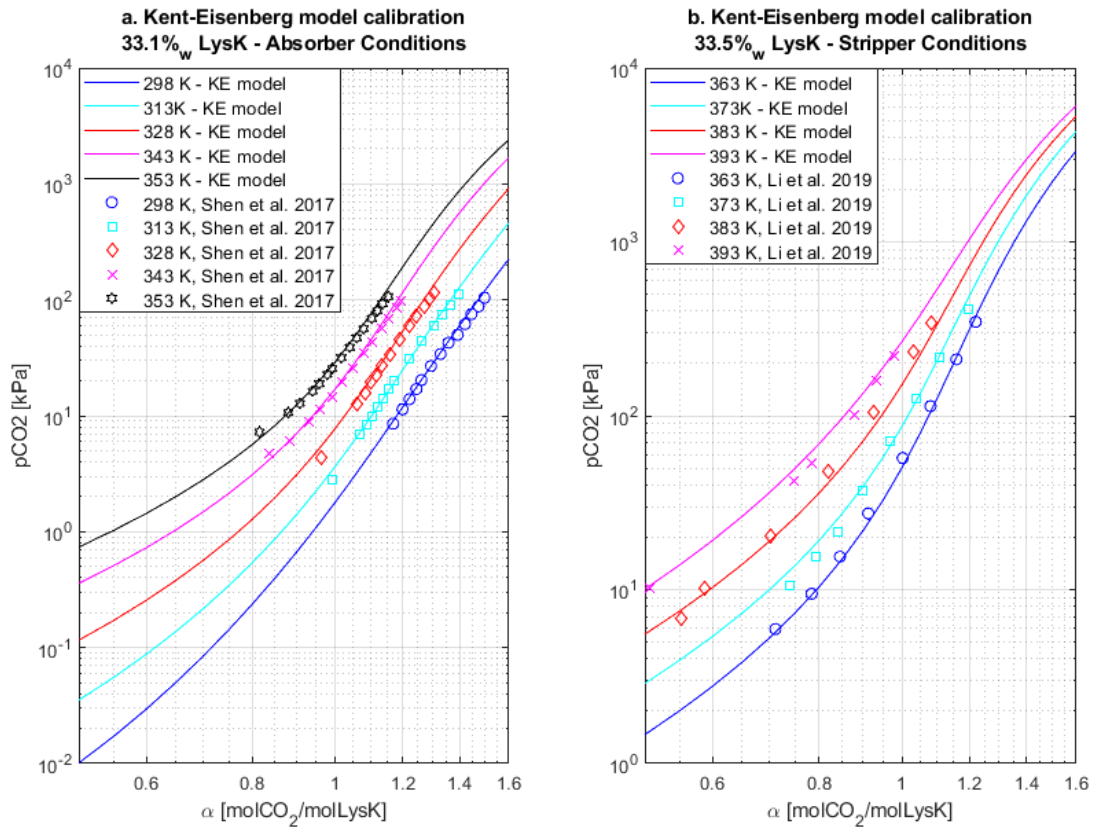
328 While developing KE model, coefficients of carbamate hydrolysis reactions ( $K_{R1}$ ,  $K_{R2}$ ) have been adjusted  
329 over 33.1 and 33.5%<sub>w/w</sub> potassium lysinate-VLE data described in Section 3, setting CO<sub>2</sub> hydrolysis ( $K_{CO_2}$ ),  
330 bicarbonate dissociation ( $K_{HCO_3^-}$ ) and water dissociation ( $K_{H_2O}$ ) coefficients from the literature. AAS  
331 dissociation constants have been identified by interpolating experimental data from Nagai et al.<sup>53</sup> in a  
332 temperature range spanning from 283.1 K to 333.1 K; this implies that the models (both KE and DM)

333 extrapolates values of the aforementioned equilibrium constants due to the high temperature range for  
 334 calibration. Table 2 reports the complete set of coefficients and associated temperature range; information  
 335 comes both from the literature – with references – and Kent-Eisenberg correlation developed in this work.

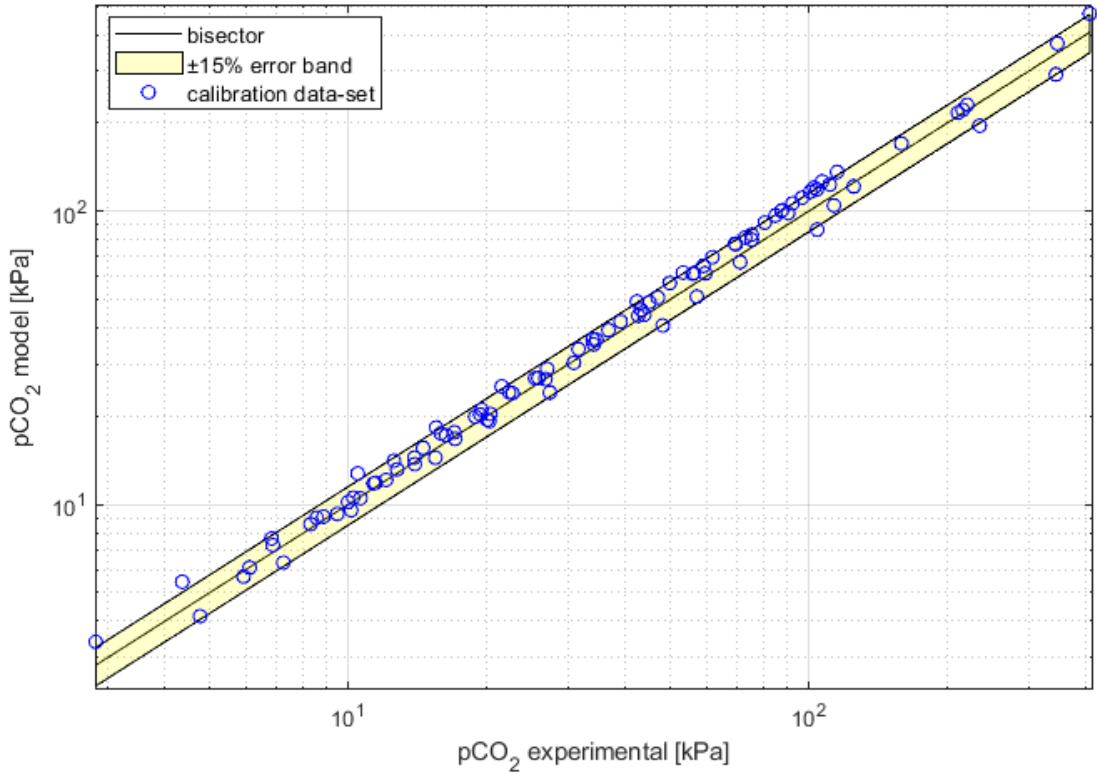
336 Table 2: Proposed equilibrium constants for the LysK/CO<sub>2</sub>/H<sub>2</sub>O system as a function of temperature (molal base).

Constant (Molality based)	Functional form: $\ln(K_i) = a + \frac{b}{T} + c \ln(T) + dT + \frac{e}{T^2}$					$\Delta T$ [°C]	Notes
	a	b	c	d	e		
$K_{R1}$	7.7594E-01	-8.0245E+02	0	0	0	25-120	Present work – regressed with revised KE
$K_{R2}$	1.2759E+01	-4.3795E+03	0	0	0	25-120	Present work – regressed with revised KE
$K_{LysH^+}$	-3.5851E+01	0	0	5.0100E-02	0	10-60	Data interpolated from Nagai et al. <sup>53</sup>
$K_{LysH}$	-1.2193E+02	0	1.7032E+01	0	0	10-60	Data interpolated from Nagai et al. <sup>53</sup>
$K_{CO_2}$	-1.2030E+03	6.8359E+04	1.8844E+02	-2.0642E-01	-4.7129E+06	0-400	63
$K_{HCO_3^-}$	1.7536E+02	-7.2306E+03	-3.0651E+01	1.3148E-02	-3.7281E+05	0-250	63
$K_{H_2O}$	1.409E+02	-1.3445E+04	-2.2477E+01	0	0	0-225	63,64

337  
 338 The revised Kent-Eisenberg model fits the experimental data from Shen et al. and Li et al. at 33.1 and 33.5  
 339 %<sub>w/w</sub> aqueous LysK solution adequately (see Figure 5), showing better accuracy in the middle loading range.  
 340 The model (AAD = 9%) embeds an activity coefficient correction from Debye-Hückel, which provides a  
 341 more accurate theoretical foundation, steering extrapolation. The parity plot is reported in Figure 6,  
 342 highlighting 15% error bar between model response and experimental data.



343  
 344 Figure 5: Results of the revised KE model representing CO<sub>2</sub> solubility in a. 33.1%w/w and b. 33.5%w/w LysK aqueous solution.



345

346  
347

Figure 6: Parity plot representative of the results of the revised KE model for CO<sub>2</sub> solubility in 33.1 and 33.5%w/w LysK aqueous solution.

348  
349  
350  
351  
352  
353

KE is an empirical correlation used for data fitting. Within this work, KE has paved the ground for the implementation of the Deshmukh-Mather model. Given the lack of complete CO<sub>2</sub> VLE data, extrapolation with KE is supported by the activity coefficients from Debye–Hückel, preserving physical significance in the solubility profiles (p<sub>CO<sub>2</sub></sub> vs. loading isotherms at different temperatures). From the analysis of the dataset, it stands out that future VLE experimental campaigns should measure CO<sub>2</sub> solubility in aqueous LysK over complete loading range (0.1-1.5 molCO<sub>2</sub>/molLysK), allowing proper DM calibration.

354  
355  
356  
357  
358  
359  
360  
361  
362  
363  
364  
365  
366

Data fitting provided by the revised KE model is appropriate and most of the model results fall within a ±15% error bar (Figure 6). Despite the introduction of activity coefficients in the revised Kent-Eisenberg, the correlation remains an empirical model, developed to fill the literature gap, mainly consisting in the lack of selected equilibrium constants for the LysK/CO<sub>2</sub>/H<sub>2</sub>O system. To set the ground for further breakthroughs providing independently-measured and validated equilibrium constants, and working towards a valid and thermodynamically-sound model, a complete Deshmukh-Mather model is proposed in the present study. The model contains temperature-dependent parameters (e.g., Henry coefficient, equilibrium constants, Debye-Hückel term in the activity coefficient expression) and composition-dependent non-ideality is also included in the Guggenheim equation, which relies on both ionic strength and individual constituent molalities (Paragraph 2.4). DM model has been calibrated against the same dataset used for KE calibration, regressing binary interaction coefficients in Matlab<sup>®</sup> (fminsearch function, objective function from Eq. 19). Adjusted Ion-ion, ion-molecule and molecule-molecule interaction parameter values selected according to Weiland et al.<sup>62</sup> (see Section 3) are reported in Table 3.

367  
368

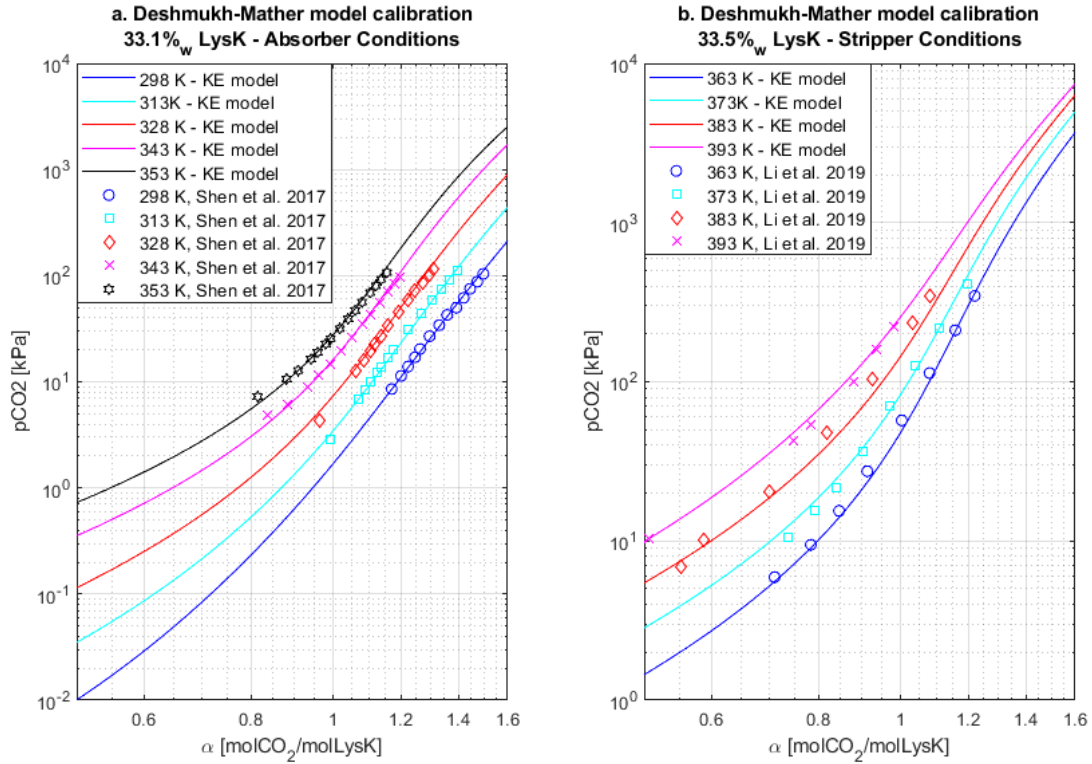
Table 3: Species interactions and regressed binary interaction parameters.

INTERACTIONS	a <sub>ij</sub> [kgH <sub>2</sub> O/kmol ]	b <sub>ij</sub> [kgH <sub>2</sub> O/kmolK ]
LysH <sup>+</sup> /NH <sub>3</sub> <sup>+</sup> – R <sub>2</sub> R <sub>1</sub> CH – NH <sub>2</sub>	3.8616e+00	-1.6345e-01
LysH <sup>+</sup> /NH <sub>2</sub> – R <sub>2</sub> R <sub>1</sub> CH – NH <sub>2</sub>	5.4588e-01	-1.1619e+00
LysH <sup>+</sup> /HCO <sub>3</sub> <sup>-</sup>	1.7302e+00	-2.8313e-02
LysH <sup>+</sup> / CO <sub>3</sub> <sup>2-</sup>	2.8097e-01	-1.3054e+00

$\text{Lys}^-/\text{Lys}^-$	1.2424e+00	2.8589e-02
$\text{Lys}^-/\text{NH}_3^+ - \text{R}_2\text{R}_1\text{CH} - \text{NH}_2$	-1.1361e-01	-1.0827e-01
$\text{Lys}^-/\text{NH}_2 - \text{R}_2\text{R}_1\text{CH} - \text{NH}_2$	7.9814e-01	4.8883e-01
$\text{Lys}^-/\text{HCO}_3^-$	-1.5917e+00	-1.4828e+00

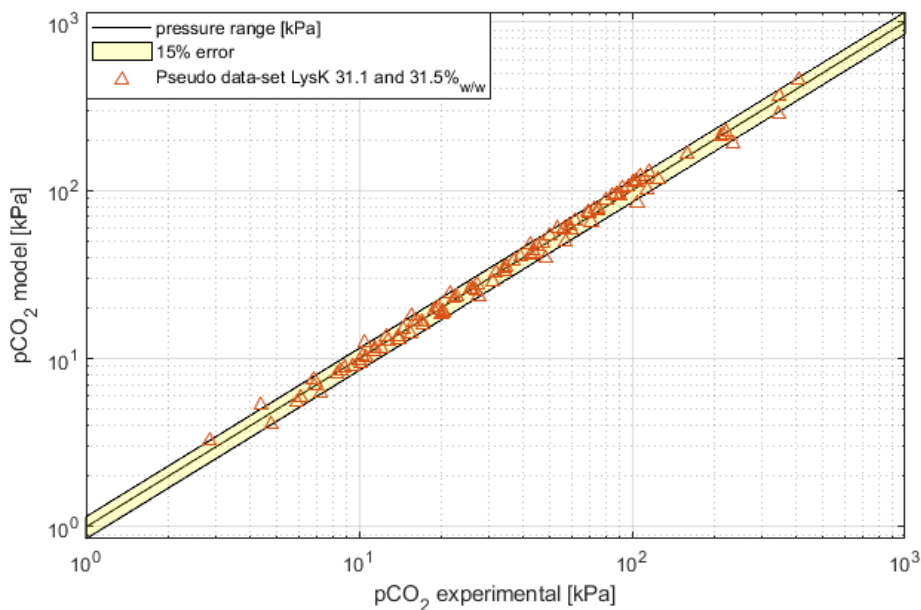
369  
370  
371  
372  
373

Figure 7 reports equilibrium isotherms of the DM model obtained after calibration (AAD = 7%), with related parity plot in Figure 8. Figure 9 shows speciation for a 33%w/w aqueous LysK system at 313.2 K. In Figure 10, DM model validation is represented.



374  
375

Figure 7: Deshmukh-Mather model representing  $\text{CO}_2$  solubility in 33.1 and 33.5%w/w aqueous LysK solution.



376  
377  
378

Figure 8: DM parity plot -  $\text{CO}_2$  solubility in 33.1 and 33.5%w/w LysK aqueous solution.

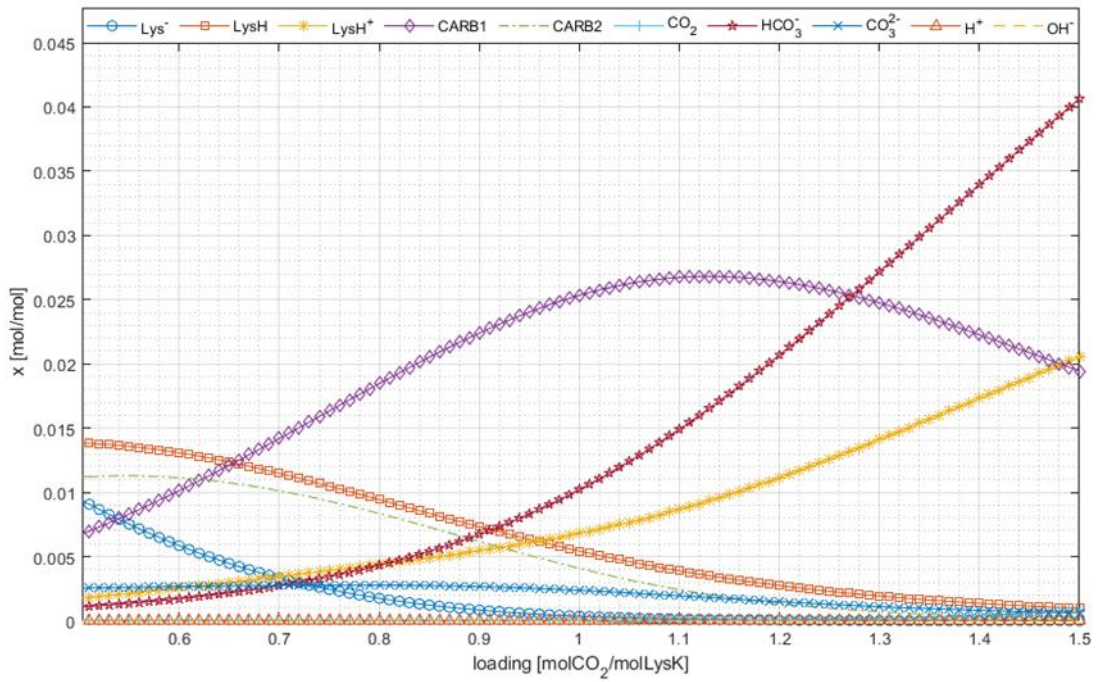


Figure 9: Speciation for 33.1%<sub>w/w</sub> aqueous LysK solution and 313.2K.

380  
381

382

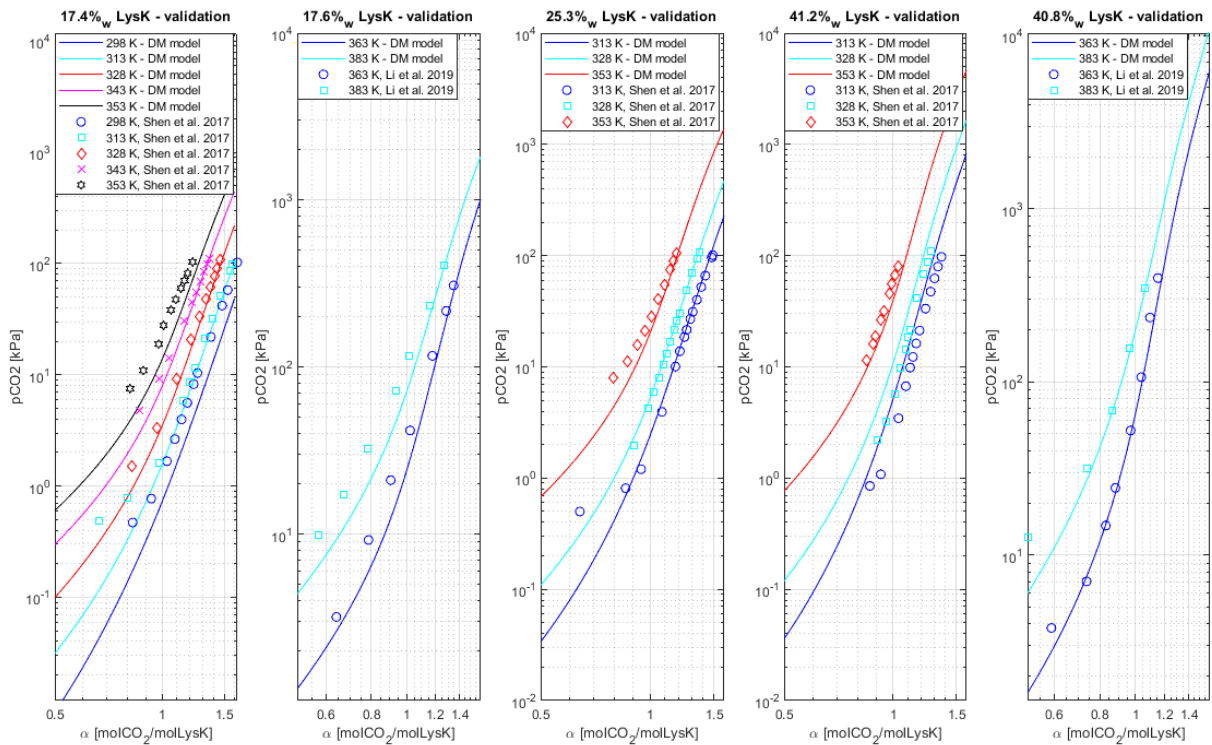


Figure 10: Solubility from DM model – validation for different selected solubility data.

383

384

385 Higher model deviation at low partial pressure can be attributed to the higher relative experimental error  
 386 underlined by the data providers<sup>44</sup>: below 1 kPa, the recorded partial pressure of CO<sub>2</sub> is comparable with the  
 387 maximum error provided by the pressure transducer (0.25 kPa) used during the test campaign. Moreover, the



388 overall standard uncertainty affecting the reported values of experimental CO<sub>2</sub> partial pressure is equal to  
389 1.50 kPa<sup>44</sup>, which significantly affects the accuracy of data at this order of magnitude (1 kPa). This also  
390 explains the scarcity of experimental data at such low partial pressures.

391

392 DM model properly fits the experimental data, showing slightly better accuracy than KE correlation (AAD -  
393 DM= 7%). An analysis of the Deshmukh-Mather outcome shows how the prediction accuracy is higher with  
394 respect to KE for medium-to-high CO<sub>2</sub> partial pressures. This trend is coherent with the addition of a short-  
395 range interaction term in the activity coefficient expression, which mainly rectifies the Henry's coefficient to  
396 account for non-ideality, with significant effects at high loadings.

397

## 398 5. Conclusions and perspectives

399 Potassium lysinate is being addressed as a solvent of interest in the field of post combustion capture of CO<sub>2</sub>.  
400 The design of related absorption units operating with amino acid salts solutions is under investigation from  
401 both academia and industry. Absorption/stripping unit sizing and full process optimization require a reliable  
402 description of the thermodynamic system, developing accurate models to reproduce CO<sub>2</sub> solubility in LysK  
403 solutions.

404 A significant literature gap undermining the description of the LysK/CO<sub>2</sub>/H<sub>2</sub>O system exists because of the  
405 lack of carbamate hydrolysis equilibrium constants and in the limited data available for AAS protonation  
406 equilibrium constants. Moreover, limited loading range investigated in vapour-liquid equilibrium  
407 experiments for model regression, validation, and CO<sub>2</sub> solubility description in the selected solution as well  
408 as concerns on VLE data consistency can be highlighted after literature analysis.

409 The present work tackles the limits of the current state-of-the-art, implementing: (i) a revised Kent-Eisenberg  
410 correlation defined and endowed with Debye-Hückel activity coefficient model. The Kent-Eisenberg  
411 approach provides a set of equilibrium constant coefficients calculated via experimental data regression, and  
412 the Debye-Hückel activity coefficient model allows possible extrapolation of CO<sub>2</sub> solubility below the  
413 experimental loading range; (ii) starting from the equilibrium constant functions and identified VLE  
414 calibration dataset (p<sub>CO2</sub> vs. loading) defined in point (i), a semi-empirical and thermodynamically-sound  
415 Deshmukh-Mather model has been defined and regressed against VLE data in the temperature range of  
416 298.2-393.0 K already used for KE calibration. The activity coefficient model of Deshmukh-Mather is based  
417 on the Guggenheim equation.

418 Kent-Eisenberg and Deshmukh-Mather have been calibrated over data at 33.1%<sub>w/w</sub> 33.5%<sub>w/w</sub> aqueous LysK  
419 concentrations. CO<sub>2</sub> partial pressure prediction results in an average absolute deviation equal to 9% and 7%  
420 respectively, with reference to the experimental data used for calibration. Deshmukh-Mather relies on  
421 equilibrium constants provided by Kent-Eisenberg with a computational approach consisting in VLE data  
422 regression. However, it constitutes a first rigorous, semi-empirical model which can be improved upon  
423 availability of further experimental data. Moreover, DM theoretical foundations support its adoption beyond  
424 the calibration window.

425 Within this framework, future work should focus on expanding the available experimental VLE data to  
426 describe CO<sub>2</sub> solubility in a wide loading envelope. Equilibrium constants for carbamate hydrolysis reactions  
427 should be estimated based on measurements of e.g., NRM speciation. Also, additional experimental data  
428 should be provided to characterize equilibria for AAS protonation in a wider temperature range. The new  
429 experimental information both in terms of equilibrium constants and solubility should be used together with  
430 the currently available datasets to recalibrate and validate the Deshmukh-Mather model, avoiding the use of  
431 Kent-Eisenberg as a first step to complete the set of equilibrium constant. Lastly, modelling results should be  
432 compared against other widely adopted models such as e-NRTL.

433

434 **ACKNOWLEDGEMENT**

435 Author Antonio Conversano is grateful to Laboratorio Energia e Ambiente Piacenza - LEAP s.c.a r.l. for its  
436 support during the research work.

437

438

439 **List of symbols**

440	A	limit slope of Debye–Hückel
441	a	activity
442	D <sub>s</sub>	solvent dielectric constant
443	f	fugacity (MPa)
444	F	Faraday constant (=eNA) (Cmol <sup>-1</sup> )
445	H	Henry constant (Pa kg of water mol <sup>-1</sup> )
446	K	equilibrium constant
447	I	ionic force
448	LysK	potassium lysinate
449	m	molality (mol kg <sup>-1</sup> of water)
450	P	total pressure (Pa)
451	r	ionic radius (Å)
452	R	the gas constant (JK <sup>-1</sup> mol <sup>-1</sup> )
453	T	temperature (K)
454	T <sub>R</sub>	reduced temperature (T/T <sub>C</sub> )
455	v	partial molar volume (cm <sup>3</sup> mol <sup>-1</sup> )
456	x	molar fraction in the liquid phase
457	y	molar fraction in the vapor phase
458	z	charge (C)
459	Z	compressibility factor

460

461 **Greek letters**

462	α	loading (molCO <sub>2</sub> /molLysK)
463	β <sub>ij</sub>	interaction parameter
464	ε <sub>0</sub>	vacuum permittivity
465	φ	fugacity coefficient
466	a	activity coefficient
467	ω	acentric factor

468

469 **Superscripts, subscripts, notation**

470	exp	experimental
471	i,j	component
472	l	liquid phase
473	model	model result
474	obj	objective
475	v	vapour phase
476	..	molal base
477	^	mixture
478	∞	infinite dilution

479

480

481 **BIBLIOGRAPHY**

482

- 483 (1) IEA. *Global Energy & CO<sub>2</sub> Status Report*; 2019.
- 484 (2) IEA. *Energy Technology Perspectives 2020*; 2020.
- 485 (3) Wang, M.; Lawal, A.; Stephenson, P.; Sidders, J.; Ramshaw, C. Post-Combustion CO<sub>2</sub> Capture with  
486 Chemical Absorption: A State-of-the-Art Review. *Chem. Eng. Res. Des.* **2011**, 89 (9), 1609–1624.  
487 <https://doi.org/10.1016/j.cherd.2010.11.005>.
- 488 (4) van Os, P. *CESAR-CO<sub>2</sub> Enhanced Separation and Recovery*; 2006; Vol. 4.
- 489 (5) CaESAR. *European Best Practice Guidelines for Assessment of CO<sub>2</sub> Capture Technologies*; 2011.
- 490 (6) Cremona, R.; Delgado, S.; Valtz, A.; Conversano, A.; Gatti, M.; Coquelet, C. Density and Viscosity  
491 Measurements and Modeling of CO<sub>2</sub>-Loaded and Unloaded Aqueous Solutions of Potassium  
492 Lysinate. *J. Chem. Eng. Data* **2021**, 66 (12), 4460–4475. <https://doi.org/10.1021/acs.jced.1c00520>.

- 493 (7) Budzianowski, W. M. *Energy Efficient Solvents for CO<sub>2</sub> Capture by Gas-Liquid Absorption*;  
494 Budzianowski, W. M., Ed.; Green Energy and Technology; Springer International Publishing: Cham,  
495 2017. <https://doi.org/10.1007/978-3-319-47262-1>.
- 496 (8) Sang Sefidi, V.; Luis, P. Advanced Amino Acid-Based Technologies for CO<sub>2</sub> Capture: A Review.  
497 *Ind. Eng. Chem. Res.* **2019**, *58* (44), 20181–20194. <https://doi.org/10.1021/acs.iecr.9b01793>.
- 498 (9) Jockenhövel, T.; Schneider, R. Towards Commercial Application of a Second-Generation Post-  
499 Combustion Capture Technology — Pilot Plant Validation of the Siemens Capture Process and  
500 Implementation of a First Demonstration Case. *Energy Procedia* **2011**, *4*, 1451–1458.  
501 <https://doi.org/10.1016/j.egypro.2011.02.011>.
- 502 (10) Conversano, A. *Thermodynamic Modelling and Process Design of a CO<sub>2</sub> Capture Unit with Amino  
503 Acid Salts Solutions for Combined Cycle Decarbonisation*; Politecnico di Milano - PhD Thesis, 2021.
- 504 (11) Conversano, A.; Porcu, A.; Mureddu, M.; Pettinau, A.; Gatti, M. Bench-Scale Experimental Tests and  
505 Data Analysis on CO<sub>2</sub> Capture with Potassium Prolinate Solutions for Combined Cycle  
506 Decarbonization. *Int. J. Greenh. Gas Control* **2020**, *93*, 102881.  
507 <https://doi.org/10.1016/j.ijggc.2019.102881>.
- 508 (12) Majchrowicz, M. E.; Brillman, D. W. F. Solubility of CO<sub>2</sub> in Aqueous Potassium L-Prolinate  
509 Solutions—Absorber Conditions. *Chem. Eng. Sci.* **2012**, *72*, 35–44.  
510 <https://doi.org/https://doi.org/10.1016/j.ces.2011.12.014>.
- 511 (13) Suleman, H.; Maulud, A. S.; Man, Z. Review and Selection Criteria of Classical Thermodynamic  
512 Models for Acid Gas Absorption in Aqueous Alkanolamines. *Rev. Chem. Eng.* **2015**, *31* (6).  
513 <https://doi.org/10.1515/revce-2015-0030>.
- 514 (14) Mondal, B. K.; Bandyopadhyay, S. S.; Samanta, A. N. VLE of CO<sub>2</sub> in Aqueous Sodium Glycinate  
515 Solution – New Data and Modeling Using Kent–Eisenberg Model. *Int. J. Greenh. Gas Control* **2015**,  
516 *36*, 153–160. <https://doi.org/10.1016/j.ijggc.2015.02.010>.
- 517 (15) Aftab, A.; M. Shariff, A.; Garg, S.; Lal, B.; Shaikh, M. S.; Faiqa, N. Solubility of CO<sub>2</sub> in Aqueous  
518 Sodium β-Alaninate: Experimental Study and Modeling Using Kent Eisenberg Model. *Chem. Eng.  
519 Res. Des.* **2018**, *131*, 385–392. <https://doi.org/10.1016/j.cherd.2017.10.023>.
- 520 (16) Garg, S.; Shariff, A. M.; Shaikh, M. S.; Lal, B.; Aftab, A.; Faiqa, N. VLE of CO<sub>2</sub> in Aqueous  
521 Potassium Salt of L-Phenylalanine: Experimental Data and Modeling Using Modified Kent-Eisenberg  
522 Model. *J. Nat. Gas Sci. Eng.* **2016**, *34*, 864–872. <https://doi.org/10.1016/j.jngse.2016.07.047>.
- 523 (17) Syalsabila, A.; Maulud, A. S.; Suleman, H.; Hadi Md Nordin, N. A. VLE of Carbon Dioxide-Loaded  
524 Aqueous Potassium Salt of L -Histidine Solutions as a Green Solvent for Carbon Dioxide Capture:  
525 Experimental Data and Modelling. *Int. J. Chem. Eng.* **2019**, *2019*, 1–11.  
526 <https://doi.org/10.1155/2019/9428638>.
- 527 (18) Chang, Y.-T.; Leron, R. B.; Li, M.-H. Carbon Dioxide Solubility in Aqueous Potassium Salt  
528 Solutions of L-Proline and DL-α-Aminobutyric Acid at High Pressures. *J. Chem. Thermodyn.* **2015**,  
529 *83*, 110–116. <https://doi.org/10.1016/j.jct.2014.12.010>.
- 530 (19) Chen, C.-C.; Evans, L. B. A Local Composition Model for the Excess Gibbs Energy of Aqueous  
531 Electrolyte Systems. *AIChE J.* **1986**, *32* (3), 444–454. <https://doi.org/10.1002/aic.690320311>.
- 532 (20) Deshmukh, R. D.; Mather, A. E. A Mathematical Model for Equilibrium Solubility of Hydrogen  
533 Sulfide and Carbon Dioxide in Aqueous Alkanolamine Solutions. *Chem. Eng. Sci.* **1981**, *36* (2), 355–  
534 362. [https://doi.org/10.1016/0009-2509\(81\)85015-4](https://doi.org/10.1016/0009-2509(81)85015-4).
- 535 (21) Moioli, S.; Ho, M. T.; Wiley, D. E.; Pellegrini, L. A. Thermodynamic Modeling of the System of  
536 CO<sub>2</sub> and Potassium Taurate Solution for Simulation of the Carbon Dioxide Capture Process. *Chem.  
537 Eng. Res. Des.* **2018**, *136*, 834–845. <https://doi.org/10.1016/j.cherd.2018.06.032>.
- 538 (22) Orlov, A. A.; Valtz, A.; Coquelet, C.; Rozanska, X.; Wimmer, E.; Marcou, G.; Horvath, D.; Poulain,  
539 B.; Varnek, A.; de Meyer, F. Computational Screening Methodology Identifies Effective Solvents for  
540 CO<sub>2</sub> Capture. *Commun. Chem.* **2022**, *5* (1), 37. <https://doi.org/10.1038/s42004-022-00654-y>.
- 541 (23) Suleman, H.; Maulud, A. S.; Fosbøl, P. L.; Nasir, Q.; Nasir, R.; Shahid, M. Z.; Nawaz, M.;  
542 Abunowara, M. A Review of Semi-Empirical Equilibrium Models for CO<sub>2</sub>-Alkanolamine-H<sub>2</sub>O  
543 Solutions and Their Mixtures at High Pressure. *J. Environ. Chem. Eng.* **2021**, *9* (1), 104713.  
544 <https://doi.org/10.1016/j.jece.2020.104713>.
- 545 (24) Renon, H.; Prausnitz, J. M. Local Compositions in Thermodynamic Excess Functions for Liquid  
546 Mixtures. *AIChE J.* **1968**, *14* (1), 135–144. <https://doi.org/10.1002/aic.690140124>.
- 547 (25) Pitzer, K. S. Electrolytes. From Dilute Solutions to Fused Salts. *J. Am. Chem. Soc.* **1980**, *102* (9),  
548 2902–2906. <https://doi.org/10.1021/ja00529a006>.

- 549 (26) Gregor, H. P. *Electrolyte Solutions*. R. A. Robinson and R. H. Stokes. Academic Press, New York,  
550 1959. Xv + 559 Pp. \$11.50. *J. Appl. Polym. Sci.* **1960**, 3 (8), 255–255.  
551 <https://doi.org/10.1002/app.1960.070030823>.
- 552 (27) Austgen, D. M.; Rochelle, G. T.; Peng, X.; Chen, C. C. Model of Vapor-Liquid Equilibria for  
553 Aqueous Acid Gas-Alkanolamine Systems Using the Electrolyte-NRTL Equation. *Ind. Eng. Chem.*  
554 *Res.* **1989**, 28 (7), 1060–1073. <https://doi.org/10.1021/ie00091a028>.
- 555 (28) N. Borhani, T.; Nabavi, S. A.; Hanak, D. P.; Manovic, V. Thermodynamic Models Applied to CO 2  
556 Absorption Modelling. *Rev. Chem. Eng.* **2020**. <https://doi.org/10.1515/revce-2019-0058>.
- 557 (29) Plaza, J. M.; Wagener, D. Van; Rochelle, G. T. Modeling CO2 Capture with Aqueous  
558 Monoethanolamine. *Energy Procedia* **2009**, 1 (1), 1171–1178.  
559 <https://doi.org/10.1016/j.egypro.2009.01.154>.
- 560 (30) Thomsen, K.; C. Iliuta, M.; Rasmussen, P. Extended UNIQUAC Model for Correlation and  
561 Prediction of Vapor–Liquid–Liquid–Solid Equilibria in Aqueous Salt Systems Containing Non-  
562 Electrolytes. Part B. Alcohol (Ethanol, Propanols, Butanols)–Water–Salt Systems. *Chem. Eng. Sci.*  
563 **2004**, 59 (17), 3631–3647. <https://doi.org/10.1016/j.ces.2004.05.024>.
- 564 (31) Aronu, U. E.; Gondal, S.; Hessen, E. T.; Haug-warberg, T.; Hartono, A.; Hoff, K. A.; Svendsen, H. F.  
565 Solubility of CO 2 in 15 , 30 , 45 and 60 Mass % MEA from 40 to 120 1 C and Model Representation  
566 Using the Extended UNIQUAC Framework. *Chem. Eng. Sci.* **2011**, 66 (24), 6393–6406.  
567 <https://doi.org/10.1016/j.ces.2011.08.042>.
- 568 (32) Faramarzi, L.; Kontogeorgis, G. M.; Thomsen, K.; Stenby, E. H. Thermodynamic Modeling of the  
569 Solubility of CO2 in Aqueous Alkanolamine Solutions Using the Extended UNIQUAC Model  
570 Application to Monoethanolamine and Methyl-diethanolamine. *Energy Procedia* **2009**, 1 (1), 861–  
571 867. <https://doi.org/10.1016/j.egypro.2009.01.114>.
- 572 (33) Fredenslund, A.; Jones, R. L.; Prausnitz, J. M. Group-Contribution Estimation of Activity  
573 Coefficients in Nonideal Liquid Mixtures. *AIChE J.* **1975**, 21 (6), 1086–1099.  
574 <https://doi.org/10.1002/aic.690210607>.
- 575 (34) Ye, K.; Freund, H.; Sundmacher, K. Modelling (Vapour+liquid) and (Vapour+liquid+liquid)  
576 Equilibria of {water (H2O)+methanol (MeOH)+dimethyl Ether (DME)+carbon Dioxide (CO2)}  
577 Quaternary System Using the Peng–Robinson EoS with Wong–Sandler Mixing Rule. *J. Chem.*  
578 *Thermodyn.* **2011**, 43 (12), 2002–2014. <https://doi.org/10.1016/j.jct.2011.07.016>.
- 579 (35) Pahlavanzadeh, H.; Nourani, S.; Saber, M. Experimental Analysis and Modeling of CO2 Solubility in  
580 AMP (2-Amino-2-Methyl-1-Propanol) at Low CO2 Partial Pressure Using the Models of Deshmukh–  
581 Mather and the Artificial Neural Network. *J. Chem. Thermodyn.* **2011**, 43 (12), 1775–1783.  
582 <https://doi.org/10.1016/j.jct.2011.05.032>.
- 583 (36) Mai Lerche, B. *CO 2 Capture from Flue Gas Using Amino Acid Salt Solutions*; 2012.
- 584 (37) Shen, S.; Yang, Y.; Wang, Y.; Ren, S.; Han, J.; Chen, A. CO2 Absorption into Aqueous Potassium  
585 Salts of Lysine and Proline: Density, Viscosity and Solubility of CO2. *Fluid Phase Equilib.* **2015**,  
586 399, 40–49. <https://doi.org/10.1016/j.fluid.2015.04.021>.
- 587 (38) Shen, S.; Yang, Y.; Bian, Y.; Zhao, Y. Kinetics of CO 2 Absorption into Aqueous Basic Amino Acid  
588 Salt: Potassium Salt of Lysine Solution. *Environ. Sci. Technol.* **2016**, 50 (4), 2054–2063.  
589 <https://doi.org/10.1021/acs.est.5b04515>.
- 590 (39) Conversano, A.; Porcu, A.; Mureddu, M.; Pettinau, A.; Gatti, M. Bench-Scale Absorption Testing of  
591 Aqueous Potassium Lysinate as a New Solvent for CO2 Capture in Natural Gas-Fired Power Plants.  
592 *Int. J. Greenh. Gas Control* **2021**, 106, 103268. <https://doi.org/10.1016/j.ijggc.2021.103268>.
- 593 (40) Nelson, D. L. (David L.; Cox, M. M. *Lehninger Principles of Biochemistry*; Fourth edition. New  
594 York : W.H. Freeman, 2005., 2005.
- 595 (41) Guo, C.; Holland, G. P. Investigating Lysine Adsorption on Fumed Silica Nanoparticles. *J. Phys.*  
596 *Chem. C* **2014**, 118 (44), 25792–25801. <https://doi.org/10.1021/jp508627h>.
- 597 (42) Kitadai, N.; Yokoyama, T.; Nakashima, S. ATR-IR Spectroscopic Study of L-Lysine Adsorption on  
598 Amorphous Silica. *J. Colloid Interface Sci.* **2009**, 329 (1), 31–37.  
599 <https://doi.org/10.1016/j.jcis.2008.09.072>.
- 600 (43) Nolting, D.; Aziz, E. F.; Ottosson, N.; Faubel, M.; Hertel, I. V.; Winter, B. PH-Induced Protonation  
601 of Lysine in Aqueous Solution Causes Chemical Shifts in X-Ray Photoelectron Spectroscopy. *J. Am.*  
602 *Chem. Soc.* **2007**, 129 (45), 14068–14073. <https://doi.org/10.1021/ja0729711>.
- 603 (44) Shen, S.; Zhao, Y.; Bian, Y.; Wang, Y.; Guo, H.; Li, H. CO2 Absorption Using Aqueous Potassium  
604 Lysinate Solutions: Vapor – Liquid Equilibrium Data and Modelling. *J. Chem. Thermodyn.* **2017**,

- 115, 209–220. <https://doi.org/10.1016/j.jct.2017.07.041>.
- 605  
606 (45) Kent, R. L.; Elsenberg, B. BETTER DATA FOR AMINE TREATING. *Hydrocarbon Processing*.  
607 1976, pp 87–90.
- 608 (46) Jou, F. Y.; Mather, A. E.; Otto, F. D. Solubility of Hydrogen Sulfide and Carbon Dioxide in Aqueous  
609 Methyldiethanolamine Solutions. *Ind. Eng. Chem. Process Des. Dev.* **1982**, *21* (4), 539–544.  
610 <https://doi.org/10.1021/i200019a001>.
- 611 (47) Hu, W.; Chakma, A. Modelling of Equilibrium Solubility of CO<sub>2</sub> and H<sub>2</sub>S in Aqueous Amino  
612 Methyl Propanol (AMP) Solutions. *Chem. Eng. Commun.* **1990**, *94* (1), 53–61.  
613 <https://doi.org/10.1080/00986449008911455>.
- 614 (48) Hu, W.; Chakma, A. Modelling of Equilibrium Solubility of CO<sub>2</sub> and H<sub>2</sub>S in Aqueous  
615 Diglycolamine (DGA) Solutions. *Can. J. Chem. Eng.* **1990**, *68* (3), 523–525.  
616 <https://doi.org/10.1002/cjce.5450680327>.
- 617 (49) Li, M.-H.; Shen, K.-P. Calculation of Equilibrium Solubility of Carbon Dioxide in Aqueous Mixtures  
618 of Monoethanolamine with Methyldiethanolamine. *Fluid Phase Equilib.* **1993**, *85*, 129–140.  
619 [https://doi.org/10.1016/0378-3812\(93\)80008-B](https://doi.org/10.1016/0378-3812(93)80008-B).
- 620 (50) Haji-Sulaiman, M. Z.; Aroua, M. K.; Benamor, A. Analysis of Equilibrium Data of CO<sub>2</sub> in Aqueous  
621 Solutions of Diethanolamine (DEA), Methyldiethanolamine (MDEA) and Their Mixtures Using the  
622 Modified Kent Eisenberg Model. *Chem. Eng. Res. Des.* **1998**, *76* (8), 961–968.  
623 <https://doi.org/10.1205/026387698525603>.
- 624 (51) Chakma, A.; Meisen, A. Improved Kent-Eisenberg Model for Predicting CO<sub>2</sub> Solubilities in Aqueous  
625 Diethanolamine (DEA) Solutions. *Gas Sep. Purif.* **1990**, *4* (1), 37–40. [https://doi.org/10.1016/0950-](https://doi.org/10.1016/0950-4214(90)80025-G)  
626 [4214\(90\)80025-G](https://doi.org/10.1016/0950-4214(90)80025-G).
- 627 (52) Li, C.; Zhao, Y.; Shen, S. Aqueous Potassium Lysinate for CO<sub>2</sub> Capture: Evaluating at Desorber  
628 Conditions. *Energy & Fuels* **2019**, *33* (10), 10090–10098.  
629 <https://doi.org/10.1021/acs.energyfuels.9b02659>.
- 630 (53) Nagai, H.; Kuwabara, K.; Carta, G. Temperature Dependence of the Dissociation Constants of  
631 Several Amino Acids. *J. Chem. Eng. Data* **2008**, *53* (3), 619–627. <https://doi.org/10.1021/je700067a>.
- 632 (54) Thomsen, K. Aqueous Electrolytes Model Parameters and Process Simulation, 1997.  
633 <https://doi.org/10.11581/dtu>.
- 634 (55) Guggenheim, E. A.; Stokes, R. H. Activity Coefficients of 2 : 1 and 1 : 2 Electrolytes in Aqueous  
635 Solution from Isopiestic Data. *Trans. Faraday Soc.* **1958**, *54*, 1646.  
636 <https://doi.org/10.1039/tf9585401646>.
- 637 (56) Suleman, H.; Maulud, A. S.; Syalsabila, A. Thermodynamic Modelling of Carbon Dioxide Solubility  
638 in Aqueous Amino Acid Salt Solutions and Their Blends with Alkanolamines. *J. CO<sub>2</sub> Util.* **2018**, *26*,  
639 336–349. <https://doi.org/10.1016/j.jcou.2018.05.014>.
- 640 (57) Zhao, Y.; Shen, S.; Bian, Y.; Yang, Y. nan; Ghosh, U. CO<sub>2</sub> Solubility in Aqueous Potassium  
641 Lysinate Solutions at Absorber Conditions. *J. Chem. Thermodyn.* **2017**, *111*, 100–105.  
642 <https://doi.org/10.1016/j.jct.2017.03.024>.
- 643 (58) Suleman, H.; Fosbøl, P. L. Physicochemical Data of Carbonic-Anhydrase-Blended Aqueous  
644 Potassium Lysinate Solutions as New Absorbents. *J. Chem. Eng. Data* **2020**, *65* (5), 2383–2391.  
645 <https://doi.org/10.1021/acs.jced.9b00963>.
- 646 (59) Zhao, Y.; Bian, Y.; Li, H.; Guo, H.; Shen, S.; Han, J.; Guo, D. A Comparative Study of Aqueous  
647 Potassium Lysinate and Aqueous Monoethanolamine for Postcombustion CO<sub>2</sub> Capture. *Energy &*  
648 *Fuels* **2017**, *31* (12), 14033–14044. <https://doi.org/10.1021/acs.energyfuels.7b02800>.
- 649 (60) Suleman, H.; Maulud, A. S.; Man, Z. Carbon Dioxide Solubility in Aqueous Potassium Lysinate  
650 Solutions: High Pressure Data and Thermodynamic Modeling. *Procedia Eng.* **2016**, *148*, 1303–1311.  
651 <https://doi.org/10.1016/j.proeng.2016.06.543>.
- 652 (61) Mazinani, S.; Ramazani, R.; Samsami, A.; Jahanmiri, A.; Van der Bruggen, B.; Darvishmanesh, S.  
653 Equilibrium Solubility, Density, Viscosity and Corrosion Rate of Carbon Dioxide in Potassium  
654 Lysinate Solution. *Fluid Phase Equilib.* **2015**, *396*, 28–34.  
655 <https://doi.org/10.1016/j.fluid.2015.03.031>.
- 656 (62) Weiland, R. H.; Chakravarty, T.; Mather, A. E. Solubility of Carbon Dioxide and Hydrogen Sulfide  
657 in Aqueous Alkanolamines. *Ind. Eng. Chem. Res.* **1993**, *32* (7), 1419–1430.  
658 <https://doi.org/10.1021/ie00019a016>.
- 659 (63) Kamps, Á. P.-S.; Balaban, A.; Jödecke, M.; Kuranov, G.; Smirnova, N. A.; Maurer, G. Solubility of  
660 Single Gases Carbon Dioxide and Hydrogen Sulfide in Aqueous Solutions of N -

- 661           Methyldiethanolamine at Temperatures from 313 to 393 K and Pressures up to 7.6 MPa: New  
662           Experimental Data and Model Extension. *Ind. Eng. Chem. Res.* **2001**, *40* (2), 696–706.  
663           <https://doi.org/10.1021/ie000441r>.
- 664   (64)   Jakobsen, J. P.; Krane, J.; Svendsen, H. F. Liquid-Phase Composition Determination in  
665           CO<sub>2</sub>–H<sub>2</sub>O–Alkanolamine Systems: An NMR Study. *Ind. Eng. Chem. Res.* **2005**, *44* (26), 9894–  
666           9903. <https://doi.org/10.1021/ie048813+>.  
667